

**NANO REVIEW**

**Open Access**

# Improvement in dielectric and mechanical performance of $\text{CaCu}_{3.1}\text{Ti}_4\text{O}_{12.1}$ by addition of $\text{Al}_2\text{O}_3$ nanoparticles

Chompoonuch Warangkanagool<sup>1</sup> and Gobwute Rujijanagul<sup>2\*</sup>

## Abstract

The properties of  $\text{CaCu}_{3.1}\text{Ti}_4\text{O}_{12.1}$  [CC3.1TO] ceramics with the addition of  $\text{Al}_2\text{O}_3$  nanoparticles, prepared via a solid-state reaction technique, were investigated. The nanoparticle additive was found to inhibit grain growth with the average grain size decreasing from approximately 7.5  $\mu\text{m}$  for CC3.1TO to approximately 2.0  $\mu\text{m}$  for the unmodified samples, while the Knoop hardness value was found to improve with a maximum value of 9.8 GPa for the 1 vol.%  $\text{Al}_2\text{O}_3$  sample. A very high dielectric constant  $> 60,000$  with a low loss tangent (approximately 0.09) was observed for the 0.5 vol.%  $\text{Al}_2\text{O}_3$  sample at 1 kHz and at room temperature. These data suggest that nanocomposites have a great potential for dielectric applications.

**Keywords:** nanocomposites, dielectric properties, microstructure, mechanical property

## Background

$\text{CaCu}_3\text{Ti}_4\text{O}_{12}$  [CCTO] is an interesting dielectric material which exhibits a high dielectric constant over 10,000 at room temperature and shows temperature independence over the temperature range from approximately 100 to 400 K [1-3]. Since the discovery of this material by Subramanian et al. [1], CCTO has been widely studied to further understand and improve its properties. The CCTO crystal has a cubic symmetry with an Im3 space group. In the CCTO lattice, the  $\text{TiO}_6$  octahedra are tilted which results in a doubling of the perovskite-like structure, involved in the planar square arrangement of the oxygen around the copper ions [4]. The CCTO ceramics exhibit an electrically heterogeneous structure involving mobile-charged species in terms of the Maxwell-Wagner relaxation [5]. Internal interfaces in the polycrystalline CCTO give rise to the polarization in the insulating grain boundary and at the semiconducting grains which is well explained by the internal barrier layer capacitor [IBLC] model [6,7]. To improve the dielectric properties further, many cations have been introduced into CCTO, including Co, Zr, Fe, Sc, and Nb on the B site and substitution

of La and Eu at the A site [4,8-12]. Although some of these additives resulted in a reduction of the loss tangent, most additives also reduced the dielectric constant. Fang et al. proposed that Cu stoichiometry can affect the electrical properties of the CCTO ceramics, [13] while Kwon et al. reported that both Cu- and Ti-deficient CCTO presented a higher dielectric constant than undoped CCTO [14]. Recently, many authors have reported on the properties of composites between CCTO and other materials such as  $\text{BaTiO}_3$ ,  $\text{SrTiO}_3$ ,  $\text{ZnNb}_2\text{O}_6$ , and polystyrene [15-17]. However, the properties of composites formed by adding nanocomposites to CCTO have still not been widely investigated. In the present work, a new nanocomposite system between CCTO (with non-stoichiometric composition) and  $\text{Al}_2\text{O}_3$  nanoparticles was fabricated. We demonstrate that the dielectric behavior of the composites can be significantly improved by the addition of these nanoparticles. Some other properties of the nanocomposites were also investigated and reported.

## Experimental procedure

It has been proposed that Cu stoichiometry is related to the dielectric response [13,14]. Fang et al. [13] reported that Cu-excessive CCTO samples showed improved densification and dielectric behaviors. In the present work, Cu-excessive CCTO ceramics in a composition

\* Correspondence: rujijanagul@yahoo.com

<sup>2</sup>Department of Physics and Materials Science, Faculty of Science, Chiang Mai University, Chiang Mai, 50200, Thailand

Full list of author information is available at the end of the article

of  $\text{CaCu}_{3.1}\text{Ti}_4\text{O}_{12.1}$  [CC3.1TO] were fabricated. Our studies indicate that this composition exhibited a good densification and dielectric response (data not shown). The samples were fabricated using the solid-state mixed oxide method. Reagent grade  $\text{CaCO}_3$ ,  $\text{CuO}$ , and  $\text{TiO}_2$  powders were used as starting materials. The mixture of these powders was ground for 24 h in ethanol using zirconia grinding media. The suspension was then dried and subsequently calcined at  $900^\circ\text{C}$  for 8 h with a heating rate of  $5^\circ\text{C}/\text{min}$ . The calcined CC3.1TO powders were mixed with (0.5, 1, and 2 vol.%)  $\text{Al}_2\text{O}_3$  nanoparticles (40 nm average particle size) and 1% polyvinyl alcohol [PVA] binder and were ball-milled in ethanol for 12 h using the same method as mentioned earlier. The slurry was then dried and sieved to a fine powder. The mixed powders were uniaxially pressed into pellets at a pressure of 60 MPa. The PVA binder was burnt out at  $550^\circ\text{C}$  with a heating rate of  $1^\circ\text{C}/\text{min}$ . Finally, the pellets were sintered at  $1,025^\circ\text{C}$  for 6 h with a heating rate of  $5^\circ\text{C}/\text{min}$ . The sintered pellets were investigated for phase formation by X-ray diffraction [XRD]. Density of the sintered samples was measured using the Archimedes method with distilled water as the fluid medium. The microstructures of the sintered samples were characterized using a scanning electron microscope [SEM], and the average grain size was determined using the linear intercept method. For the electrical measurement, silver paste was applied to both sides of the circular faces of the ceramics, then dried at  $600^\circ\text{C}$  for 15 min, and cooled naturally to room temperature. The dielectric constant and dielectric loss were then

measured using a LCZ meter. The mechanical properties (hardness) of various sintered samples were studied using a Knoop microhardness tester. Indentations were applied to the polished surfaces with 0.3- and 0.5-kg loads and with an indentation period of 15 s.

## Results and discussion

### Phase formation

The XRD results for the sintered ceramics containing up to 2 vol.%  $\text{Al}_2\text{O}_3$  are illustrated in Figure 1. All of the patterns were similar to the unmodified CCTO diffraction peaks and were consistent with the results reported previously [18]. The peaks of the second phases such as  $\text{Cu}_2\text{O}$  and  $\text{CuO}$  could not be observed in the XRD patterns [14]. Further, no peak was observed for the  $\text{Al}_2\text{O}_3$  phase in any of the XRD patterns. This may be due to the amount of  $\text{Al}_2\text{O}_3$  additive which was too little to be detected at the sensitivity level of the XRD instrument.

### Densification, microstructure, and hardness behavior

The plot of density as a function of  $\text{Al}_2\text{O}_3$  volume fraction is shown in Figure 2. The density slightly increased with the increasing amounts of  $\text{Al}_2\text{O}_3$  up to 0.5 vol.% and then decreased for the 2 vol.% sample. The reduction in density for the higher  $\text{Al}_2\text{O}_3$  samples suggests that the sintering mechanism of the samples was not complete. To obtain the best densification for compositions  $> 0.5$  vol.%  $\text{Al}_2\text{O}_3$ , higher sintering temperatures or longer soaking times would be required.

Figure 3 displays the SEM micrographs of the as-sintered surfaces of CC3.1TO- $\text{Al}_2\text{O}_3$  nanocomposites. An

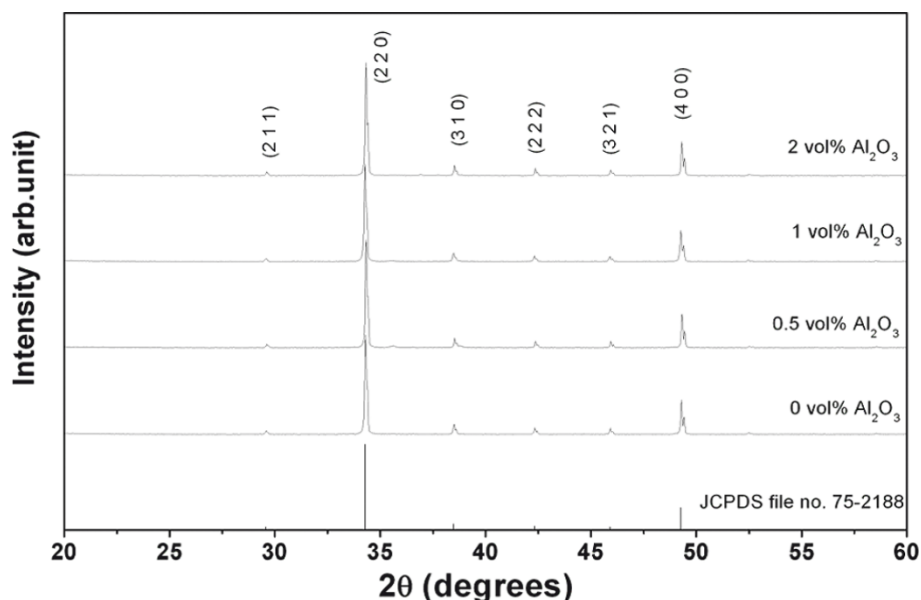


**Figure 1** XRD patterns of the surfaces of the CC3.1TO and CC3.1TO- $\text{Al}_2\text{O}_3$  pellets.

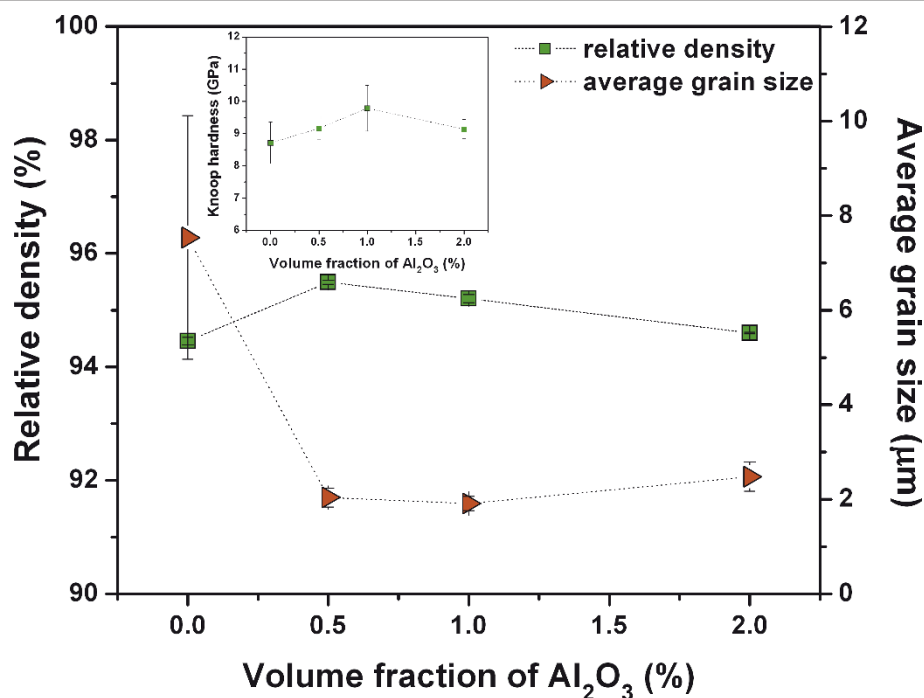


**Figure 2** Density and average grain size as Al<sub>2</sub>O<sub>3</sub> volume fraction function for CC3.1TO and CC3.1TO-Al<sub>2</sub>O<sub>3</sub> nanocomposites. Inset shows Knoop hardness value as a function of Al<sub>2</sub>O<sub>3</sub> content of the samples.

agglomeration of Al<sub>2</sub>O<sub>3</sub> nanoparticles was not explicitly observed, implying that the processing method produced a reasonably uniform distribution of the nanoparticles in the matrix of the composites. The surfaces of the CC3.1TO samples showed a duplex microstructure consisting of coarse grains (average grain size of approximately 20 μm) and fine grains (average grain size of approximately 1 μm) located around the coarse grains. This characteristic indicates an abnormal grain growth in the microstructure of the samples. The formation of a copper oxide liquid phase (in Cu-excessive CCTO), as suggested by Kim et al. [19], may be the main reason for the formation of abnormal grain growth since the present samples have a Cu-excessive CCTO composition. The liquid phase enhanced nucleation of abnormal grains and the abnormal grains were then formed after sintering. Similar results have been reported previously for Cu-excessive CCTO ceramics [14,20]. The average grain sizes of the coarse grains were found to decrease with the additive (e.g., average grain size of the coarse grains was approximately 3 μm for the 2 vol.% sample; Figure 3b). However, the average grain size of the fine grains remained unchanged for higher Al<sub>2</sub>O<sub>3</sub> content samples. Overall, the average grain size, calculated from coarse and fine grains, decreased from approximately 7.5 μm for the unmodified sample to approximately 2.0 μm for the 2 vol.% sample (Figure 2). The decrease in the average grain size is most likely caused by the

mismatch of the different components. Further, Al<sub>2</sub>O<sub>3</sub> might segregate to the grain boundaries which could prevent grain boundary movement during the sintering process and, as a result, inhibit grain growth.

The Knoop hardness values of the samples as a function of Al<sub>2</sub>O<sub>3</sub> content are illustrated in the inset of Figure 2. The Knoop hardness data reveal that the additive improved the hardness values. The maximum hardness value in this work was 9.8 GPa (for the 1 vol.% sample) which is comparable to the value reported by Puchmark et al. for the PZT-Al<sub>2</sub>O<sub>3</sub> nanocomposites. The improvement in the mechanical properties is most likely due to the nanoparticles reinforcing the grain boundaries and acting as effective pins against microcrack propagation [21]. Moreover, the enhancement of hardness can be related to the reduction in grain size, i.e., small grain size samples gave a higher measured hardness.

#### Dielectric properties

Figure 4 shows the dielectric constants versus the frequency at room temperature for the CC3.1TO and CC3.1TO-Al<sub>2</sub>O<sub>3</sub> pellets. Compared with the CC3.1TO sample, a significant improvement in the dielectric constant of the CC3.1TO-Al<sub>2</sub>O<sub>3</sub> samples was observed. For the CC3.1TO sample, the dielectric constant was 11,000 (measured at 1 kHz and at room temperature) which is close to the values reported previously [1,2]. The CC3.1TO sample also exhibited nearly dielectric-



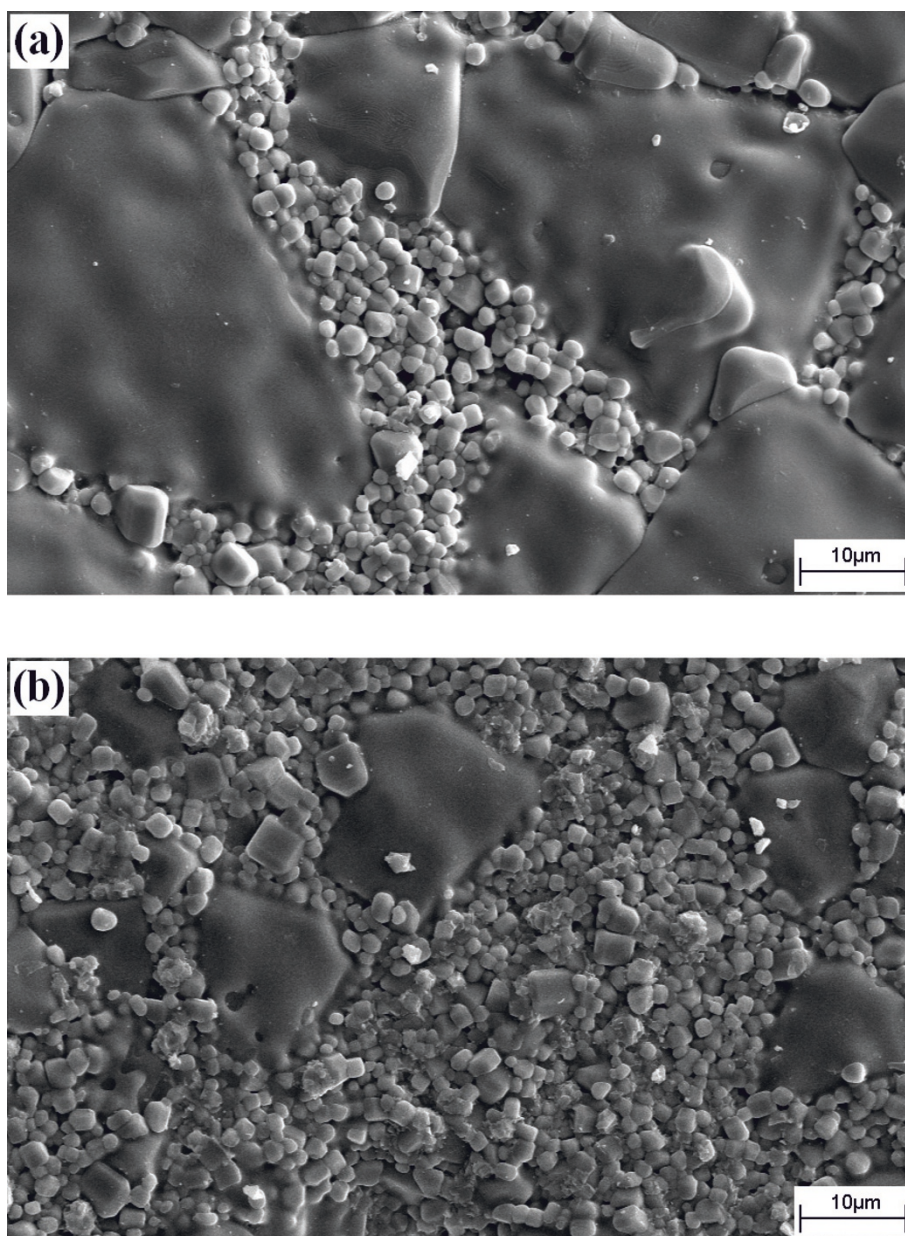


**Figure 3** SEM micrographs of as-sintered surfaces of the CC3.1TO-Al<sub>2</sub>O<sub>3</sub> nanocomposites. (a) CC3.1TO and (b) CC3.1TO and 2 vol.% Al<sub>2</sub>O<sub>3</sub>.

frequency independence over the frequency range of 0.1 to 500 kHz. Further, the dielectric constant increased reaching a value  $> 60,000$  at 1 kHz for the 0.5 vol.% sample then decreased for further increases in the Al<sub>2</sub>O<sub>3</sub> content. For the 2 vol.% sample, however, the dielectric-frequency curve showed a weak frequency dispersion of the dielectric constant. The reduction in the dielectric constant for the samples which were doped with more than 0.5 vol.% Al<sub>2</sub>O<sub>3</sub> may be due to the fact that composites with higher additive amounts (Al<sub>2</sub>O<sub>3</sub>  $>$  0.5 vol.%) also had higher structural heterogeneity.

Moreover, the formation of an impurity phase may have caused a reaction between Al<sub>2</sub>O<sub>3</sub> and CC3.1TO which could not be detected using the XRD technique [22], but it might also have contributed to the reduction in the dielectric constant. Plots of the loss tangent versus the frequency of the CC3.1TO and CC3.1TO-Al<sub>2</sub>O<sub>3</sub> pellets at room temperature are presented in the inset of Figure 4. The loss tangent-frequency curve of the CC3.1TO ceramic exhibited a weak frequency dispersion for a narrow frequency range (1 to 50 kHz). However, after adding the additive, the loss tangent significantly

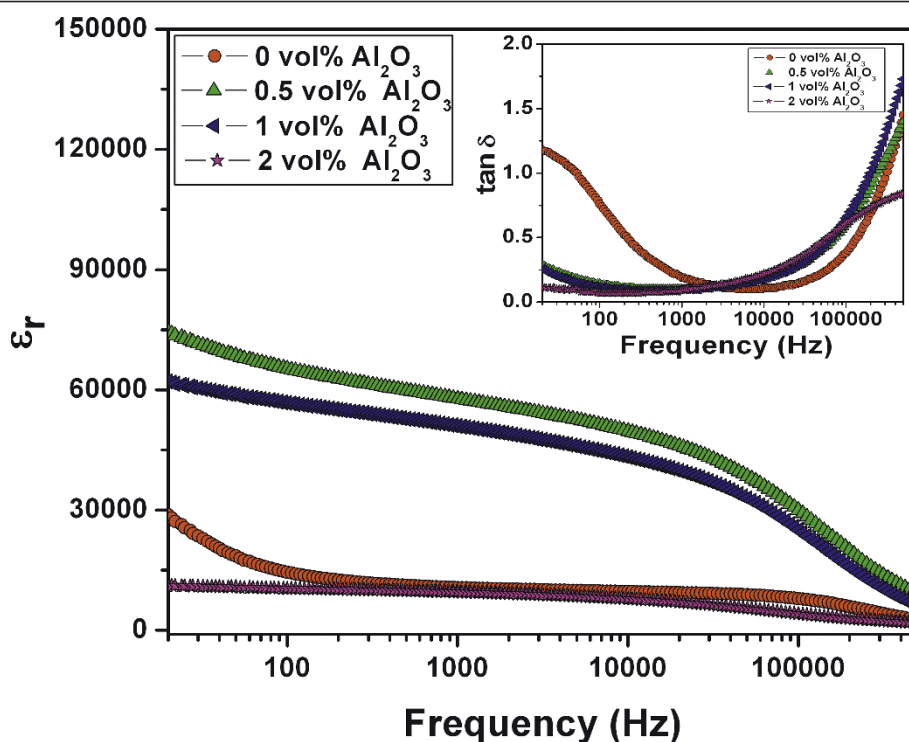


**Figure 4** Dielectric constants versus frequency at room temperature for the CC3.1TO and CC3.1TO- $\text{Al}_2\text{O}_3$  pellets. The inset shows the loss tangent versus the frequency of the ceramic pellets at room temperature.

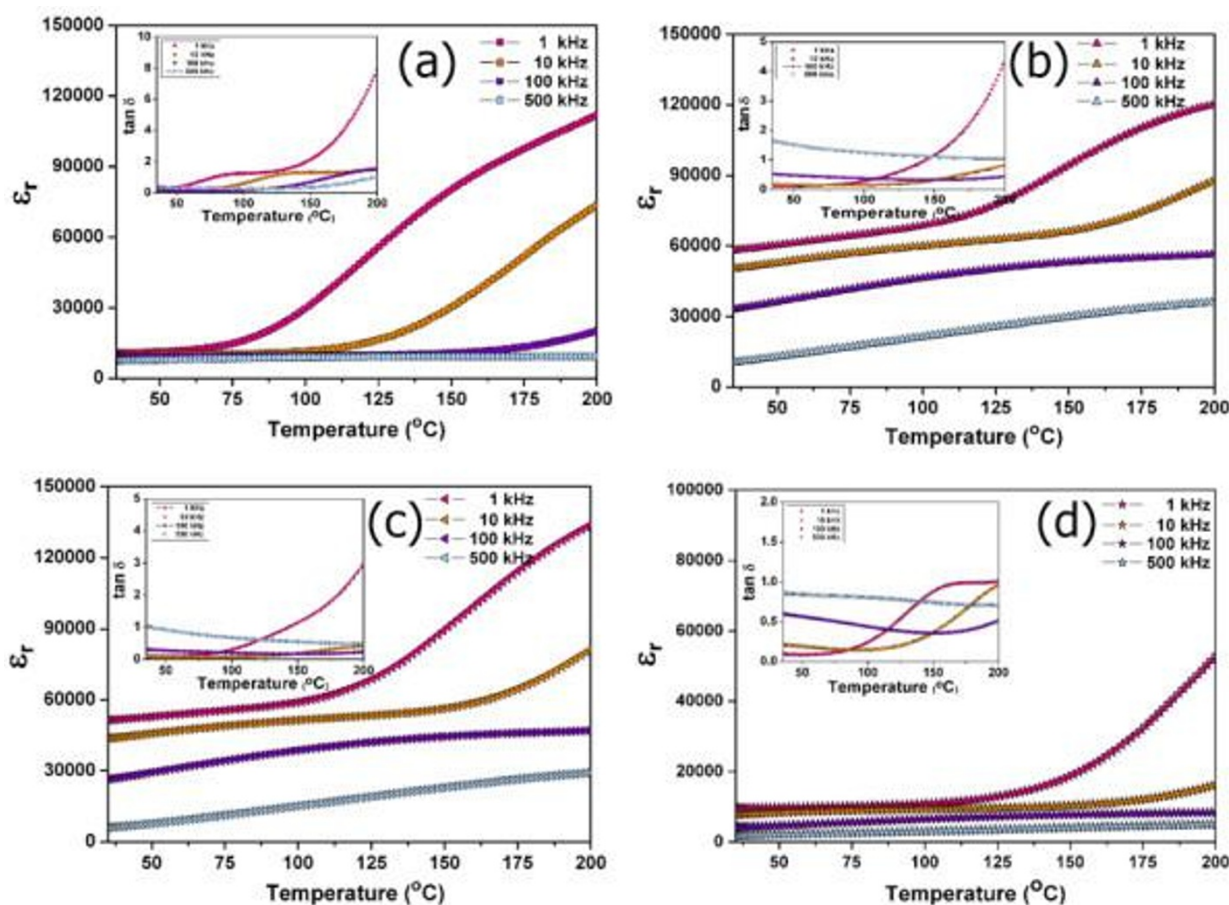
decreased at low frequencies ( $< 1$  kHz) which resulted in a wider range of frequency stability (10 Hz to 10 kHz). Further, the loss tangent decreased from 0.21 for the CC3.1TO ceramics to 0.09 for the 0.5 vol.% sample (at 1 kHz). A further slight decrease in the loss tangent was observed for additional additive amounts. The decrease in loss tangent shows a reduced conductivity of the CC3.1TO- $\text{Al}_2\text{O}_3$  samples. This result could be related to changes in the transport behavior due to an increase in resistivity at the grain boundaries where the additive nanoparticles predominantly segregated.

Figure 5 shows the dielectric constant values as a function of temperature at various frequencies for the CC3.1TO and CC3.1TO- $\text{Al}_2\text{O}_3$  pellets. The CC3.1TO sample showed a high dielectric constant ( $\epsilon_r$  approximately 10,000) with temperature and frequency stability from room temperature to  $60^\circ\text{C}$ . After adding the additive, however, a significant improvement in the dielectric behavior was observed. The 0.5 vol.% sample showed a very high dielectric constant  $> 60,000$  (at 1 kHz) which was nearly temperature-independent for the temperature range of approximately  $35^\circ\text{C}$  to  $110^\circ\text{C}$ . Compared to the CC3.1TO sample, this sample also displayed a pronounced frequency dependence of the dielectric constant especially for temperatures  $< 125^\circ\text{C}$ . Moreover, the dielectric-temperature curve of the 0.5 vol.% presented a

broad flat curve at high frequencies ( $> 10$  kHz). For higher additive amounts ( $\text{Al}_2\text{O}_3 > 0.5$  vol.%), the dielectric constant decreased with the increasing additives. Further, the dielectric frequency dispersion for the  $\text{Al}_2\text{O}_3$  nanoparticle sample with 2 vol.% was not as strong for temperatures  $< 112^\circ\text{C}$ . The loss tangent values as a function of temperature at various frequencies for the samples are illustrated in the insets of Figure 5. For the CC3.1TO sample, the loss tangent value was 0.21 and was stable with temperature as well as frequency from room temperature to approximately  $41^\circ\text{C}$ . The 0.5 vol.% sample had a loss tangent value lower than 0.10 for room temperature to approximately  $50^\circ\text{C}$ . From the (IBLC) model, the apparent dielectric constant ( $\epsilon'_r$ ) can be related to the microstructure parameters by the formula [23]:

$$\epsilon'_r = \epsilon_{\text{gb}} \left( \frac{d}{t} \right), \quad (1)$$

where  $d$  is the grain size,  $t$  is the thickness of the grain boundary (barrier width), and  $\epsilon_{\text{gb}}$  is the internal dielectric constant of the barrier material. Since the grain size of the present samples decreased with the increasing additive, Equation 1 predicts that the higher dielectric constant for the 0.5 vol.% sample is not related to the



**Figure 5** Temperature dependence of the dielectric dispersion at various frequencies. (a) CC3.1TO, (b) CC3.1TO with 0.5 vol.%  $\text{Al}_2\text{O}_3$ , (c) CC3.1TO with 1 vol.%  $\text{Al}_2\text{O}_3$ , and (d) CC3.1TO with 2 vol.%  $\text{Al}_2\text{O}_3$ .

grain size, but it may be connected to a change in the grain boundary characteristics such as  $\epsilon_{gb}$  and  $t$  after adding the additive. The reason for the change of grain boundary characteristic is still unclear, but it is possible that the  $\text{Al}_2\text{O}_3$  nanoparticles had a reaction with the matrix of the CC3.1TO, and as a result, the formation of Al-metal oxide phases at the grain boundary produced other products in small amounts which could not be detected by XRD [22]. However, the higher density for the 0.5 vol.% sample can be explained by the observed higher dielectric constant in the present work.

## Conclusions

CC3.1TO- $\text{Al}_2\text{O}_3$  nanocomposites were fabricated for the first time. The samples were prepared using a solid-state reaction. The CC3.1TO ceramics showed a duplex microstructure, consisting of coarse and fine grains, while the nanocomposites showed mainly fine grains in their microstructure due to the fact that the additive inhibited grain growth. The additive also enhanced the hardness value especially for the 1 vol.% sample.

However, the CC3.1TO and 0.5 vol.%  $\text{Al}_2\text{O}_3$  showed a high dielectric constant with a strong dielectric frequency dispersion especially at low temperatures and also had a lowered loss tangent value, as compared with other samples. These results indicate that the addition of nanoparticles may be an alternative method to improve the dielectric behavior in some other giant dielectric materials.

## Acknowledgements

This work was supported by The Thailand Research Fund (TRF), Thailand's Office of the Higher Education Commission (OHEC), and Faculty of Science and Graduate School, Chiang Mai University. The authors would like to thank Prof. Dr. Tawee Tunkasiri for his help in many facilities.

## Author details

<sup>1</sup>Department of Physics, Faculty of Science, Naresuan University, Phitsanulok, 65000, Thailand <sup>2</sup>Department of Physics and Materials Science, Faculty of Science, Chiang Mai University, Chiang Mai, 50200, Thailand

## Authors' contributions

CP carried out the fabrication of CC3.1TO, XRD characterization, SEM characterization, density measurement, grain size measurement, dielectric properties measurement, and Knoop hardness measurement. GR designed



the whole experimental procedure and related analyses. All authors read and approved the final manuscript.

#### Competing interests

The authors declare that they have no competing interests.

Received: 19 September 2011 Accepted: 5 January 2012

Published: 5 January 2012

#### References

- Subramanian MA, Li D, Duran N, Reisner BA, Sleight AW: **High dielectric constant in  $\text{ACu}_3\text{Ti}_4\text{O}_{12}$  and  $\text{ACu}_3\text{Ti}_3\text{FeO}_{12}$  phases.** *J Solid State Chem* 2000, **151**:323-325.
- Ramirez AP, Subramanian MA, Gardel M, Blumberg G, Li D, Vogt T, Shapiro SM: **Giant dielectric constant response in a copper-titanate.** *Solid State Commun* 2000, **115**:217-220.
- Homes CC, Vogt T, Shapiro SM, Wakimoto S, Ramirez AP: **Optical response of high-dielectric-constant perovskite-related oxide.** *Science* 2001, **293**:673-676.
- Leret P, Fernandez JF, de Frutos J, Fernandez-Hevia D: **Nonlinear I-V electrical behaviour of doped  $\text{CaCu}_3\text{Ti}_4\text{O}_{12}$  ceramics.** *J Eur Ceram Soc* 2007, **27**:3901-3905.
- Lunkenheimer P, Bobnar V, Pronin AV, Ritus AI, Volkov AA, Loidl A: **Origin of apparent colossal dielectric constants.** *Phys Rev B* 2002, **66**:052105.
- Sinclair DC, Adams TB, Morrison FD, West AR:  **$\text{CaCu}_3\text{Ti}_4\text{O}_{12}$ : one-step internal barrier layer capacitor.** *Appl Phys Lett* 2002, **80**:2153-2155.
- Adams TB, Sinclair DC, West AR: **Characterization of grain boundary impedances in fine- and coarse-grained  $\text{CaCu}_3\text{Ti}_4\text{O}_{12}$  ceramics.** *Adv Mater* 2002, **14**:1321-1323.
- Chung SY, Lee SI, Choi JH, Choi SY: **Initial cation stoichiometry and Q2 current-voltage behavior in Sc-doped calcium copper titanate.** *Appl Phys Lett* 2006, **89**:191907.
- Kwon S, Huang CC, Patterson EA, Cann DP: **The effect of  $\text{Cr}_2\text{O}_3$ ,  $\text{Nb}_2\text{O}_5$  and  $\text{ZrO}_2$  doping on the dielectric properties of  $\text{CaCu}_3\text{Ti}_4\text{O}_{12}$ .** *Mater Lett* 2008, **62**:633-636.
- Li T, Chen Z, Chang F, Hao J, Zhang J: **The effect of  $\text{Eu}_2\text{O}_3$  doping on  $\text{CaCu}_3\text{Ti}_4\text{O}_{12}$  varistor properties.** *J Alloy Compd* 2009, **484**:718-722.
- Chiodelli G, Massarotti V, Capsoni D, Bini M, Azzoni CB, Mozzati MC, Lupotto P: **Electric and dielectric properties of pure and doped  $\text{CaCu}_3\text{Ti}_4\text{O}_{12}$  perovskite materials.** *Solid State Commun* 2004, **132**:241-246.
- Feng L, Tang X, Yan Y, Chen X, Jiao Z, Cao G: **Decrease of dielectric loss in  $\text{CaCu}_3\text{Ti}_4\text{O}_{12}$  ceramics by La doping.** *Phys Status Solidi A* 2006, **203**:R22-R24.
- Fang TT, Mei LT, Ho HF: **Effects of Cu stoichiometry on the microstructures, barrier-layer structures, electrical conduction, dielectric responses, and stability of  $\text{CaCu}_3\text{Ti}_4\text{O}_{12}$ .** *Acta Mater* 2006, **54**:2867-2875.
- Kwon S, Huang CC, Subramanian MA, Cann DP: **Effects of cation stoichiometry on the dielectric properties of  $\text{CaCu}_3\text{Ti}_4\text{O}_{12}$ .** *J Alloy Compd* 2009, **473**:433-436.
- Almeida AFL, Fachine PBA, Góes JC, Valente MA, Miranda MAR, Sombra ASB: **Dielectric properties of  $\text{BaTiO}_3$  (BTO)- $\text{CaCu}_3\text{Ti}_4\text{O}_{12}$  (CCTO) composite screen-printed thick films for high dielectric constant devices in the medium frequency (MF) range.** *Mater Sci Eng B* 2004, **111**:113-123.
- Yu H, Liu H, Hao H, Luo D, Cao M: **Dielectric properties of  $\text{CaCu}_3\text{Ti}_4\text{O}_{12}$  ceramics modified by  $\text{SrTiO}_3$ .** *Mater Lett* 2008, **62**:1353-1355.
- Du G, Li W, Fu Y, Chen N, Yin C, Yan M: **An investigation on the solid-state reactions in  $\text{CaCu}_3\text{Ti}_4\text{O}_{12}$ - $\text{ZnNb}_2\text{O}_6$  system.** *Mater Res Bull* 2008, **43**:2504-2508.
- Ni L, Chen XM, Liu XQ, Hou RZ: **Microstructure-dependent giant dielectric response in  $\text{CaCu}_3\text{Ti}_4\text{O}_{12}$  ceramics.** *Solid State Commun* 2006, **139**:45-50.
- Kim KM, Lee JH, Lee KM, Kim DY, Riu DH, Lee SB: **Microstructural evolution and dielectric properties of Cu-deficient and Cu-excess  $\text{CaCu}_3\text{Ti}_4\text{O}_{12}$  ceramics.** *Mater Res Bull* 2008, **43**:284-291.
- Shao SF, Zhang JL, Zheng P, Wang CL: **Effect of Cu-stoichiometry on the dielectric and electric properties in  $\text{CaCu}_3\text{Ti}_4\text{O}_{12}$  ceramics.** *Solid State Commun* 2007, **142**:281-286.
- Puchmark C, Rujijanagul G, Jiansirisomboon S, Tunkasiri T, Vittayakorn N, Comyn TP, Milne SJ: **Mechanical property evaluation of PZT/ $\text{Al}_2\text{O}_3$  composites prepared by a solid state mixed oxide method.** *Curr Appl Phys* 2006, **6**:323-326.
- Puchmark C, Jiansirisomboon S, Rujijanagul G, Comyn TP, He JY, Milne SJ: **Properties of lead zirconate-alumina 'Nanocomposites'.** *Mater Res Bull* 2007, **42**:1269-1277.
- Zuo R, Feng L, Yan Y, Chen B, Cao G: **Observation of giant dielectric constant in  $\text{CdCu}_3\text{Ti}_4\text{O}_{12}$  ceramics.** *Solid State Commun* 2006, **138**:91-94.

doi:10.1186/1556-276X-7-68

**Cite this article as:** Warangkanagool and Rujijanagul: Improvement in dielectric and mechanical performance of  $\text{CaCu}_{3.1}\text{Ti}_4\text{O}_{12.1}$  by addition of  $\text{Al}_2\text{O}_3$  nanoparticles. *Nanoscale Research Letters* 2012 **7**:68.

**Submit your manuscript to a SpringerOpen<sup>®</sup> journal and benefit from:**

- Convenient online submission
- Rigorous peer review
- Immediate publication on acceptance
- Open access: articles freely available online
- High visibility within the field
- Retaining the copyright to your article

Submit your next manuscript at ► [springeropen.com](http://springeropen.com)